
Understanding Contrastive Learning Through the Lens of Margins

Daniel Rho
KT

TaeSoo Kim
KT, Sungkyunkwan University

Sooill Park
Hyundai Mobis

Jaehyun Park
NC Soft

JaeHan Park
KT

Abstract

Self-supervised learning, or SSL, holds the key to expanding the usage of machine learning in real-world tasks by alleviating heavy human supervision. Contrastive learning and its varieties have been SSL strategies in various fields. We use margins as a stepping stone for understanding how contrastive learning works at a deeper level and providing potential directions to improve representation learning. Through gradient analysis, we found that margins scale gradients in three different ways: emphasizing positive samples, de-emphasizing positive samples when angles of positive samples are wide, and attenuating the diminishing gradients as the estimated probability approaches the target probability. We separately analyze each and provide possible directions for improving SSL frameworks. Our experimental results demonstrate that these properties can contribute to acquiring better representations, which can enhance performance in both seen and unseen datasets.

1 Introduction

Self-supervised learning (SSL), or unsupervised learning, has attracted a lot of attention, succeeding in a range of fields, including natural language processing and computer vision [35, 29, 14]. Self-supervised pretraining frameworks, in particular, have significantly improved several task performances by leveraging the abundance of data [14, 16, 22, 18]. Among the various SSL frameworks, contrastive learning [35, 29] is one of the universal SSL frameworks [29] not relying on domain-specific assumptions. Pretraining frameworks based on contrastive learning have been applied in various fields, ranging from the image domain [20, 5, 3, 17] to the audio domain [29, 22].

Similar to contrastive learning, face and speaker recognition tasks also adopt cosine similarity and softmax loss-based losses [39, 23, 27, 24, 2, 13]. To improve identification accuracy, these domain usually exploit margins, which are known to increase inter-class distance and decrease intra-class distance in face and speaker recognition tasks. Based on the commonality (cosine similarity and softmax loss), there have been recent attempts to benefit from the characteristic of margins in contrastive-learning-based SSL [37, 38]. These studies demonstrate that margins can improve contrastive learning-based tasks. Notwithstanding the difference between face recognition and self-supervised learning, such as the existence of class labels, the explanation of how margins work on remains solely based on the explanation from the face recognition domain.

Thus, our work starts with the following question: how do margins affect contrastive learning-based representation learning? It remains unclear how margins affect contrastive learning in the absence of class labels, which are commonly used in face recognition tasks to explain the effect of margins. Thus, our work aims to investigate how margins affect contrastive learning-based representation

learning through gradient analysis, without relying on class-based explanation. We first generalize the contrastive learning loss, specifically InfoNCE loss [29], to incorporate margins into the formulation. Then, we theoretically analyze the gradient of the generalized contrastive learning loss to identify and dissect the effect of margins on gradients.

Through gradient analysis, we found that margins affect representation learning in three ways. First, it emphasizes positive samples. Second, margins reduce the gradients of distant positive samples. Lastly, margins alleviate the slowdown effect of gradients when the estimated probability approaches the target probability. Based on the analysis, we separately explored each effect. Experimental results demonstrate that these characteristics of margins can improve representation learning.

Contrastive learning is based on identity discrimination [35], relying on the idea that representations of the same identity should cluster together while those from different identities should separate. Aside from this core idea, there are a lot of potential directions for improvement. We believe that understanding how margins affect contrastive learning can provide direction for future improvement in contrastive learning and SSL, not only helping us exploit margins in contrastive learning. We hope that our work will provide insights into the search for improving SSL.

2 Related Works

2.1 Self-supervised learning

Good latent representations should cluster representations of semantically similar samples together while dispersing and uncorrelating representations of semantically dissimilar samples [21, 12, 36]. SSL, however, should learn these relationships without ground-truth semantic information. As alternatives to manual supervision, many researchers have proposed a variety of pretext tasks that can aid in comprehending semantically relevant representations, including context prediction [28, 15], in-painting [30, 4], auto-encoding [1] and masked language modeling [14]. Using pretext tasks, SSL can utilize the abundant data and improve performance without human supervision.

Contrastive learning (InfoNCE) [29], one of the pretext tasks, aims to learn instance-level relationships between samples in a self-supervised manner using a similarity function (cosine similarity) and cross-entropy. Wu et al. [35] define different views of the same image as "positive pairs," and views from different images as "negative pairs." Contrastive learning enforces neural networks to generate close representations for positive samples and distant representations for negative samples. Several InfoNCE-based SSL methods [5, 3, 17, 20, 7] have been proposed. For example, *MoCo* [20, 8, 9] proposes using a teacher model for generating different latent representations of the same samples. *SimCLR* [5, 6] demonstrated that augmentations play a critical role in contrastive learning frameworks. *BYOL* [17], another variety of InfoNCE, proposes using only positive samples.

Several works have analyzed the properties and limitations of contrastive learning [32, 38, 34, 10]. Wang & Liu [32] analyzed the role of temperature τ in contrastive learning, and found that contrastive learning focuses on nearby samples. Similarly, Zhang et al. [38] argue that contrastive learning is robust to long-tail distribution. There are additional studies to uncover the weak spots of contrastive learning. Wang et al. [34], for example, showed that contrastive learning tends to ignore non-shared information between views, resulting in performance degradation in some downstream task. Meanwhile, Chuang et al. [10] demonstrate that contrastive learning is biased and thus de-biasing contrastive learning loss can improve representation learning.

2.2 Margin softmax loss

Face and speaker recognition tasks determine whether two given samples are representations of the same identity or not, by comparing extracted feature vectors. These tasks use (cosine) similarity-based softmax loss, using known identity information as class labels during training. Margins have been a successful method for widening inter-class, or inter-identity, distance and narrowing down intra-class distance [33, 12]. To improve recognition performance, several variety of margins have been proposed, including adaptive [39, 23, 27, 24] and stochastic margins [2].

Contrastive learning loss and margin softmax loss both use cosine similarity and softmax. Thus, there have been attempts to use margins also in tasks that use contrastive learning (or InfoNCE)-based objective functions [37, 38]. To analyze which effects of margin are major contributors to improving

representation learning, we aim to understand the margin through gradient analysis. This approach allows us to separate and analyze the complex effects that margins have on contrastive learning and might provide directions for improving self-supervised representation learning.

3 Generalized Margins for Contrastive Loss

Margins — angular margin and subtractive margin — are known to increase the inter-class distance and decrease the intra-class distance [12, 33]. Previous studies [37, 38] on the use of margins for contrastive learning were restricted to particular tasks and have not thoroughly analyzed the effect of margins on representation learning. In this section, we generalize InfoNCE [29] loss in order to include margins in contrastive learning and to analyze its effect on gradients.

3.1 Generalized InfoNCE

InfoNCE loss has been a core of several SSL methods [20, 5, 3, 17]. The loss function can be represented as follows:

$$\tilde{q}_{ij} = \frac{\exp(\text{sim}(z_i, z_j)/\tau)}{\sum_{k \in \mathcal{X}} \exp(\text{sim}(z_i, z_k)/\tau)} \quad (1)$$

$$\tilde{\mathcal{L}}_i = - \sum_{j \in \mathcal{X}} p_{ij} \log \tilde{q}_{ij}. \quad (2)$$

z_i denotes a latent feature of input i . \mathcal{X} denotes the set of samples in a mini-batch, and p_{ij} denotes the target probability of two identities (i and j) being equal. $\text{sim}(\cdot, \cdot)$ is a similarity function. Given that cosine similarity is used as a similarity function, \tilde{q}_{ij} (Eq. 1) can be rewritten as follows:

$$\theta_{ij} = \arccos(\text{sim}(z_i, z_j)) \quad (3)$$

$$\tilde{\delta}_{ij} = \cos(\theta_{ij})/\tau \quad (4)$$

$$\tilde{q}_{ij} = \frac{\exp(\tilde{\delta}_{ij})}{\sum_{k \in \mathcal{X}} \exp(\tilde{\delta}_{ik})}. \quad (5)$$

θ_{ij} denotes the angle between two normalized latent features. Since this mathematical expression makes it much easier to analyze the effect of margins on representation learning, we will use this expression for the following explanations.

Other contrastive learning techniques, like BYOL [17], that exclusively use positive samples cannot be covered by Eq. 2. As a result, we generalize the equation by introducing β to the denominator of \tilde{q}_{ij} as proposed in BYOL [17]. By rewriting the equation, we get the following equation:

$$\tilde{\mathcal{L}}_i = - \sum_{j \in \mathcal{X}} p_{ij} \log \frac{\exp(\tilde{\delta}_{ij})}{\beta \sum_{k \in \mathcal{X}} \exp(\tilde{\delta}_{ik})} = - \sum_{j \in \mathcal{X}} p_{ij} \tilde{\delta}_{ij} + \beta \sum_{j \in \mathcal{X}} p_{ij} \log \sum_{k \in \mathcal{X}} \exp(\tilde{\delta}_{ik}). \quad (6)$$

If β is non-zero, the loss uses both positive and negative samples. Otherwise, only positive samples will be used for training. Therefore, this equation can generalize any contrastive learning-based SSL method, such as MoCo, SimCLR, and BYOL.

3.2 Including margins in InfoNCE

There are two types of margins; angular margin m_1 and subtractive margin m_2 . Angular margin m_1 is added to the angle between two representations θ_{ij} , and subtractive margin m_2 is subtracted to the logits. These margins are added only to positive samples. After including margins, we can rewrite the logits and the estimated probability as follows:

$$\delta_{ij} = (\cos(\theta_{ij} + m_1 p_{ij}) - m_2 p_{ij})/\tau \quad (7)$$

$$q_{ij} = \frac{\exp(\delta_{ij})}{\sum_{k \in \mathcal{X}} \exp(\delta_{ik})}. \quad (8)$$

Likewise, Eq. 6 can be rewritten as follows:

$$\mathcal{L}_i = - \sum_{j \in \mathcal{X}} p_{ij} \delta_{ij} + \beta \sum_{j \in \mathcal{X}} p_{ij} \log \sum_{k \in \mathcal{X}} \exp(\delta_{ik}). \quad (9)$$

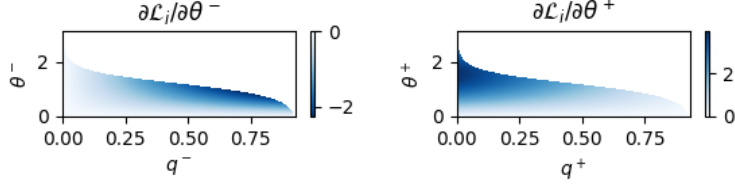


Figure 1: Gradient magnitudes of contrastive learning loss without margins (Eq. 6). β , τ , and the batch size was set to 1, 0.25, and 256, respectively. q^+ and q^- denote the estimated probability of positive and negative samples. θ^+ and θ^- refer to the angles of positive and negative samples.

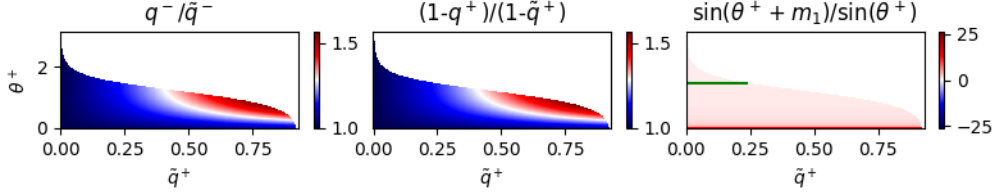


Figure 2: The visualization of gradient multiplier due to angular margin m_1 (Eq. 12). β , τ , m_1 and the batch size was set to 1, 0.25, 0.2, and 256, respectively. Non-colored areas represent impossible combination of \tilde{q}^+ and θ^+ . The leftmost figure illustrates the multiplier map for negative samples ($p = 0$), while two other figures shows that of positive samples ($p = 1$). The green curve on the rightmost figure indicates points where the ratio is 1.

Eq. 9 can generalize to various SSL methods, including MoCo, SimCLR and BYOL by simply setting margins to zeros. By analyzing the gradient of Eq. 9, we can identify the following three characteristics of margins (m_1 and m_2):

- m_1 emphasizes positive samples.
- m_1 affects the curvature of the positive sample gradient scale.
- m_1 and m_2 attenuate diminishing gradients as q_{ij} approaches p_{ij} .

We will describe how we get these characteristics of margins and how they works in detail in the following sections (Secs. 4 and 5).

4 Gradient Analysis

In order to examine how margins affect representation learning, we analyze the derivative of Eqs. 6 and 9 with respect to the angle θ_{ij} . For consistency, we will use notations j and k for arbitrary indices, and notations l and h for positive and negative sample indices, respectively.

The derivative of $\tilde{\mathcal{L}}_i$ (Eq. 6) and \mathcal{L}_i (Eq. 9) with respect to θ_{ij} can be represented as follows:

$$\frac{\partial \tilde{\mathcal{L}}_i}{\partial \theta_{ij}} = \frac{\partial \tilde{\mathcal{L}}_i}{\partial \tilde{\delta}_{ij}} \frac{\partial \tilde{\delta}_{ij}}{\partial \theta_{ij}} = (p_{ij} - \beta \tilde{q}_{ij}) \frac{\sin(\theta_{ij})}{\tau} \quad (10)$$

$$\frac{\partial \mathcal{L}_i}{\partial \theta_{ij}} = \frac{\partial \mathcal{L}_i}{\partial \delta_{ij}} \frac{\partial \delta_{ij}}{\partial \theta_{ij}} = (p_{ij} - \beta q_{ij}) \frac{\sin(\theta_{ij} + m_1 p_{ij})}{\tau} \quad (11)$$

Before analyzing the margin effects, we first discuss the gradient of InfoNCE loss without margins (Eq. 10). Fig. 1 illustrates that the magnitude of gradient diminishes as the angle θ_{ij} approaches zero. Additionally, the magnitude diminishes as the estimated probabilities q_{ij} of both positive and negative samples approach their target probabilities p_{ij} .

The following equation shows the relationship between the gradient without margins (Eq. 10) and the gradient with margins (Eq. 11):

$$\frac{\partial \mathcal{L}_i}{\partial \theta_{ij}} = \frac{\partial \tilde{\mathcal{L}}_i}{\partial \theta_{ij}} \cdot \frac{p_{ij} - \beta q_{ij}}{p_{ij} - \beta \tilde{q}_{ij}} \cdot \frac{\sin(\theta_{ij} + m_1 p_{ij})}{\sin(\theta_{ij})} \quad (12)$$

This equation shows that margins scale gradients through two terms; $(p_{ij} - \beta q_{ij}) / (p_{ij} - \beta \tilde{q}_{ij})$ and $\sin(\theta_{ij} + m_1 p_{ij}) / \sin(\theta_{ij})$. The angular margin m_1 affects the gradient through $(p_{ij} - \beta q_{ij}) / (p_{ij} - \beta \tilde{q}_{ij})$ and $\sin(\theta_{ij} + m_1 p_{ij}) / \sin(\theta_{ij})$, while subtractive margin only works through $(p_{ij} - \beta q_{ij}) / (p_{ij} - \beta \tilde{q}_{ij})$. We will analyze how each margin affects gradients through these two terms in the following subsections.

4.1 Angular margin

The angular margin m_1 multiplies the gradient of a negative sample $\partial \tilde{\mathcal{L}}_i / \partial \theta_{ih}$ by q_{ih} / \tilde{q}_{ih} . For a positive sample l , the angular margin m_1 multiplies the gradient of a positive sample $\partial \tilde{\mathcal{L}}_i / \partial \theta_{il}$ by $\sin(\theta_{il} + m_1) / \sin(\theta_{il})$. If β is non-zero, the positive sample gradient is also multiplied by $(1 - q_{il}) / (1 - \tilde{q}_{il})$.

Fig. 2 visualizes these three terms; q_{ih} / \tilde{q}_{ih} , $(1 - q_{il}) / (1 - \tilde{q}_{il})$, and $\sin(\theta_{il} + m_1) / \sin(\theta_{il})$. The figure illustrates three key characteristics. First, the scale of positive sample gradients drastically increases due to $\sin(\theta_{il} + m_1) / \sin(\theta_{il})$. Second, the gradient of a positive sample significantly diminishes as the angle θ_{il} widens due to $\sin(\theta_{il} + m_1) / \sin(\theta_{il})$. That is, the angular margin m_1 forces neural networks to focus on positive samples with small angles. Although $(1 - q_{il}) / (1 - \tilde{q}_{il})$ can reduce the magnitude when θ_{il} approaches zero, its impact is relatively minor. Lastly, the angular margin m_1 scales up the gradient as the estimated probability of a positive sample approaches the target probability. This effect counteracts the phenomenon observed in Fig. 1, where the gradient diminishes as an estimated probability q_{ij} gets closer to its target probability p_{ij} . Yet, since this attenuating factor is solely dependent on positive samples, we analyze the attenuation effect and coupled scaling scheme separately in Sec. 5.4.

4.2 Subtractive margin

The subtractive margin m_2 directly suppresses the logits of positive samples δ_{il} . To better understand how the subtractive margin works, we reformulate $\exp(\delta_{ij})$ as follows:

$$\exp(\delta_{ij}) = \exp\left(\frac{\cos(\theta_{ij} + m_1 p_{ij}) - m_2 p_{ij}}{\tau}\right) = \exp\left(\frac{\cos(\theta_{ij} + m_1 p_{ij})}{\tau}\right) \exp\left(-\frac{m_2 p_{ij}}{\tau}\right). \quad (13)$$

This equation shows that using the subtractive margin m_2 equals multiplying original exponential of logits by $\exp(-m_2 p_{ij} / \tau)$. Assuming β is 1 and p_{ij} is either zero or one, $\partial \mathcal{L}_i / \partial \theta_{ij}$ can be expressed as follows:

$$\frac{\partial \mathcal{L}_i}{\partial \theta_{ij}} = (p_{ij} - \tilde{q}_{ij}) \cdot \frac{\sin(\theta_{ij} + m_1 p_{ij})}{\tau} \cdot \frac{1}{(1 - (1 - \exp(-m_2 / \tau)) \tilde{q}_{ij})}, \quad (14)$$

where \tilde{q}_{il} denotes the estimated probability of a positive sample l without margins. The proof of this is addressed in the supplementary. As Eq. 14 shows, the subtractive margin m_2 scales the original gradient (one without m_2) by $1 / (1 - (1 - \exp(-m_2 / \tau)) \tilde{q}_{il})$. Given that $1 / (1 - (1 - \exp(-m_2 / \tau)) \tilde{q}_{il})$ increases as \tilde{q}_{il} increases, m_2 gives more weight as \tilde{q}_{il} increases. Although not exactly the same, this is similar to the last characteristic of m_1 (Sec. 4.1 and Fig. 2).

If m_2 approaches infinity when β is 1, the subtractive margin totally removes the diminishing term $(p_{ij} - \beta \tilde{q}_{ij})$ of positive samples. That is, positive sample gradients become independent of the estimated probabilities and thus of other negative samples.

$$\lim_{m_2 \rightarrow \infty} \frac{\partial \mathcal{L}_i}{\partial \theta_{il}} = \frac{\sin(\theta_{il} + m_1 p_{il})}{\tau} \quad (15)$$

In short, m_2 controls the scale of attenuation. Since the gradient multiplier $1 / (1 - (1 - \exp(-m_2 / \tau)) \tilde{q}_{il})$ also affects negative samples, we analyze this effect in Sec. 5.4 in two ways: positive-sample-only and positive-sample-bound attenuation.

5 Experimental Results

We first evaluate the impact of three effects: emphasizing positive samples (Sec. 5.2), weighting positive samples differently depending on their angles (Sec. 5.3), and attenuating the diminishing gradient effect as the estimated probability of positive sample q_{il} approaches the target probability

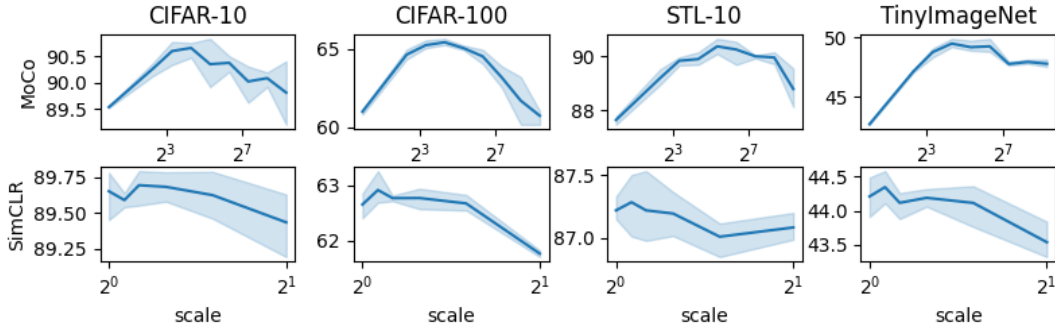


Figure 3: Top 1 accuracy when emphasizing positive samples through s (Eq. 16).

p_{il} (Sec. 5.4). To this end, we conducted separate experiments on MoCov3 [9], SimCLR [5], and BYOL [17], which all represent different SSL approaches. MoCo and BYOL both use teacher models which stabilize optimization. While BYOL only uses positive samples, MoCo and SimCLR use negative samples. These differences allowed us to observe how the three effects affect representation learning. We also compared with the baselines (MoCo, SimCLR, and BYOL) using linear probing (only tuning a linear layer on top of the frozen pretrained backbone model) and transfer learning (tuning the linear layer on different dataset) in Sec. 5.5. Our experiments utilized five different datasets, including CIFAR-10 [25], CIFAR-100 [25], STL-10 [11], TinyImageNet [26], and ImageNet [31].

5.1 Implementation details

For four datasets (CIFAR-10, CIFAR-100, STL-10, TinyImageNet), we used a modified ResNet-18 [19] as proposed by Zheng et al. [40]. We basically followed the experimental settings from ReSSL [40]. To compare with the baselines, we pretrain networks for 200 epochs and tune only a linear layer on top of the frozen pretrained backbone model for 100 epochs (linear probing). Keep in mind that our intention is to examine the three effects on SSL methods rather than to compare the performance of different SSL methods. Therefore, we fixed the training hyper-parameters across different SSL methods. To evaluate on ImageNet, we utilized ResNet-50 [19] as the backbone model, following other SSL literature [20, 5, 17]. We pretrained for 100 epochs and fine-tuned a linear layer for 90 epochs, consistent with previous works [9, 5]. We did not alter any hyperparameters of the baselines, except for newly introduced hyperparameters (s and c). Please refer to the supplementary for more detailed experimental settings due to page limits.

5.2 Emphasizing positive samples

In this section, we quantitatively measure the effect of emphasizing positive samples. To this end, we introduce a new hyper-parameter s to scale positive sample gradients as follows:

$$w_{ij} = (1 - p_{ij}) + s \cdot p_{ij} \quad (16)$$

$$\delta_{ij}^{scale} = \delta_{ij} w_{ij} + sg(\delta_{ij}) \cdot (1 - w_{ij}). \quad (17)$$

w_{ij} denotes sample-wise weight, and $sg(\cdot)$ is the stop gradient operation. We trained neural networks by replacing δ_{ij} with δ_{ij}^{scale} in Eq. 9.

We tested the effect of emphasizing positive samples on both MoCo and SimCLR. BYOL was excluded because it only uses positive samples and thus emphasizing positive samples is the same as increasing the learning rate. Fig. 3 visualizes the results. As the figure shows, scaling up positive sample gradients significantly improves the performance of MoCo. When the scale s gets too large, however, the performance gain begins to disappear. It can be seen that lowering the relative weights of negative samples can improve the performance, but if they get too small, it will rather cause performance degradation. Given that the gradients of MoCo approach those of BYOL as the scale s approaches infinity (assuming the learning rate is adjusted accordingly), the presence of negative samples may be rather necessary for better SSL performance. It is also worth noting that emphasizing positive samples yields higher accuracy than using margins in the case of MoCo (Tab. 3). This implies that the performance improvement brought by emphasizing positive samples is offset by other factors.

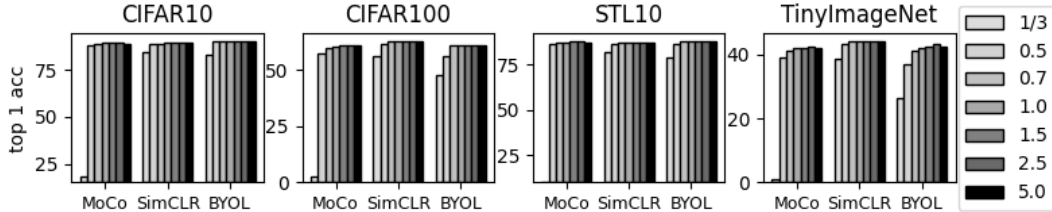


Figure 4: Controlling positive sample gradient scale curvatures through c (Eq. 19). s was set to one.

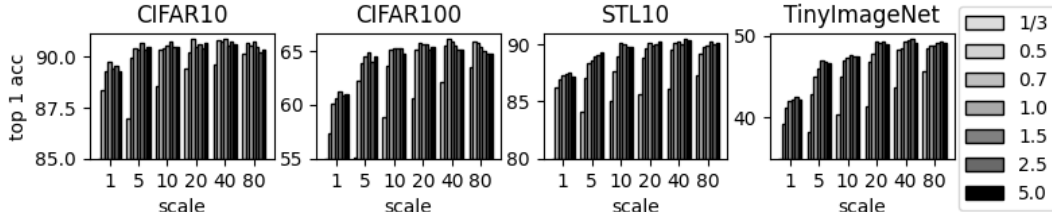


Figure 5: Controlling both scale s and curvature c of MoCo (Eq. 19).

Unlike MoCo, however, SimCLR does not significantly improve by scaling up positive sample gradients. We conjecture that this is due to a lack of a teacher model. The existence of the teacher model can prevent representations from converging at a single point [17]. Without a stabilizing component, such as a teacher model, emphasizing positive samples seems to impose a burden on the representation learning of SimCLR. From the perspective that s controls the weights of positive samples within a mini-batch, this observation reveals a pattern that aligns with the fact that SimCLR requires a large batch size [5]. Although emphasizing positive samples is not possible for all SSL methods, it is a prominent direction.

5.3 Curvature of the positive sample gradient scale

In this section, we analyze the effect of weighting positive samples differently based on their angles p_{ij} . We will refer to a weight curve, a function of the positive sample angle, as a curvature. To experiment with convex, linear, and concave curvatures, we first define a curve $\gamma(x, c)$ as follows:

$$\gamma(x, c) = |(1 - x^c)^{1/c}|, \quad (18)$$

where c is a parameter to control the curvature, and $|\cdot|$ denotes the absolute operation. When c is infinity, it becomes exactly the same as not controlling the curvature at all. To use Eq. 18 to control the diminishing rate of the positive samples gradient, we set the weights as follows;

$$w_{ij}^{dim} = (1 - p_{ij}) + \gamma(\theta_{ij}/\pi, c) \cdot s \cdot p_{ij}. \quad (19)$$

For experiments, we replaced w_{ij} with w_{ij}^{dim} in Eq. 17. We used three convex (c is 1/3, 0.5, 0.7), three concave (c is 1.5, 2.5, 5), and linear (c is 1) curves.

Fig. 4 shows how different c affects various SSL methods and datasets, and Fig. 5 shows the performance of MoCo as both scale s and c change. If s is 1, unless c is extremely small, the performance variation due to c is very minimal. However, as s increases, the performance variation

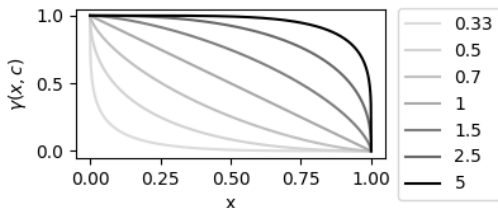


Figure 6: Illustration of $\gamma(x, c)$ (Eq. 18).

Table 1: Top 1 accuracy of ResNet-50 when linear probing on ImageNet.

	Epoch	ImageNet
MoCov3 [9]	100	68.9
+ pos. & curv.	100	70.9
SimCLR [5]	100	64.7
+ pos. & curv.	100	65.7

caused by c becomes more pronounced. While it varies slightly depending on the dataset, in many cases, c being close to or greater than 1 yields the optimal outcome. Furthermore, considering that the curvature due to margins is highly convex, this explains partly why using margins might not fully exploit the advantage of weighting positive samples differently based on their angles.

Table 2: The effect of each gradient attenuation type and attenuation magnitude α .

method	α	CIFAR10		CIFAR100		STL10		TinyImageNet	
		type I	type II	type I	type II	type I	type II	type I	type II
MoCo	0	89.413		60.956		87.629		42.133	
	0.25	89.376	89.713	60.857	61.217	87.292	87.455	42.420	42.460
	1	89.743	89.633	60.997	61.263	87.329	87.442	42.797	42.510
SimCLR	0	89.653		62.655		87.188		44.184	
	0.25	89.867	89.557	62.407	62.763	87.200	87.042	44.206	44.197
	1	89.735	89.767	62.840	62.800	87.300	87.317	44.260	44.260

Table 3: Linear probing. *pos.* denotes emphasizing positive samples and *curv.* denotes controlling the curvature of positive gradient scales.

	CIFAR10	CIFAR100	STL10	TinyImageNet
MoCo	89.413 \pm 0.109	60.956 \pm 0.167	87.629 \pm 0.175	42.133 \pm 0.225
+ margins	89.840 \pm 0.105	61.796 \pm 0.254	87.688 \pm 0.275	42.860 \pm 0.280
+ pos.	90.663 \pm 0.159	65.413 \pm 0.205	90.357 \pm 0.398	48.273 \pm 0.405
+ pos. & curv.	90.865 \pm 0.025	66.095 \pm 0.295	90.361 \pm 0.057	48.503 \pm 0.270
SimCLR	89.653 \pm 0.207	62.655 \pm 0.277	87.188 \pm 0.145	44.184 \pm 0.220
+ margins	90.447 \pm 0.191	63.507 \pm 0.414	87.430 \pm 0.220	44.593 \pm 0.410
+ pos.	89.695 \pm 0.150	62.917 \pm 0.302	87.284 \pm 0.248	44.348 \pm 0.295
+ pos. & curv.	90.190 \pm 0.067	63.503 \pm 0.279	87.346 \pm 0.156	44.376 \pm 0.201
BYOL	90.283 \pm 0.109	61.006 \pm 0.140	87.546 \pm 0.668	41.846 \pm 0.097
+ curv.	90.485 \pm 0.085	61.170 \pm 0.340	88.051 \pm 0.230	43.332 \pm 0.564

Table 4: Transfer learning. While freezing the pretrained backbone model, only the linear layer was tuned to the target dataset. It is expressed in the form of "pretrained dataset \rightarrow target dataset".

	CIFAR100 \rightarrow CIFAR10	CIFAR10 \rightarrow CIFAR100	TinyImageNet \rightarrow STL10	STL10 \rightarrow TinyImageNet
MoCo	75.417 \pm 0.241	43.590 \pm 0.225	72.013 \pm 0.250	31.140 \pm 0.130
+ margins	75.380 \pm 0.418	43.190 \pm 0.255	72.154 \pm 0.654	30.543 \pm 0.160
+ pos.	78.847 \pm 0.244	55.113 \pm 0.434	78.100 \pm 0.185	41.825 \pm 0.431
+ pos. & curv.	78.600 \pm 0.042	52.940 \pm 0.750	78.734 \pm 0.040	41.777 \pm 0.690
SimCLR	77.300 \pm 0.014	48.845 \pm 0.615	75.533 \pm 0.026	35.108 \pm 0.453
+ margins	76.377 \pm 0.301	47.023 \pm 0.219	75.617 \pm 0.273	34.747 \pm 0.430
+ pos.	76.893 \pm 0.220	49.090 \pm 0.262	75.675 \pm 0.194	35.067 \pm 0.380
+ pos. & curv.	76.620 \pm 0.190	48.683 \pm 0.107	75.571 \pm 0.220	34.280 \pm 0.215
BYOL	75.086 \pm 0.156	41.560 \pm 0.321	69.433 \pm 0.272	30.306 \pm 0.309
+ curv.	74.820 \pm 0.552	39.445 \pm 0.078	72.442 \pm 0.366	29.260 \pm 0.028

5.4 Attenuating the diminishing gradients

As explained in Secs. 4.1 and 4.2, margins can attenuate the diminishing gradients as q_{ij} approaches p_{ij} . This, however, is also bound to a side condition; the scale depends only on the positive sample. Thus, we ran experiments on two types of attenuation scales; type I and II.

For type I, the gradient multiplier also scales negative samples, as m_2 does (Eq. 14). Specifically, we multiply $1/(1 - \alpha\tilde{q}_{il})$ to gradients to both positive and negative samples.

$$w_{ij}^I = \sum_{k \in \mathcal{X}} \frac{p_{ik}}{1 - \alpha\tilde{q}_{ik}} \quad (20)$$

If α equals $1 - \exp(-m_2/\tau)$, type I equals using subtractive margin m_2 (Eq. 14). For type II, we only scale gradients of positive samples only as follows:

$$w_{ij}^{II} = (1 - p_{ij}) + \frac{p_{ij}}{p_{ij} - \alpha\tilde{q}_{ij}}. \quad (21)$$

Tab. 2 shows the performance as α changes. We exempt BYOL because q_{ij} cannot exist without negative samples. As the table shows, attenuating positive gradients as q_{il} approaches p_{il} does not significantly improve performance (type I), nor does de-coupling positive and negative sample weights (type II). This might be related to the fact that many face recognition methods use only the angular margin m_1 .

5.5 Comparison with baselines

In this section, we compare the baselines (MoCo, SimCLR, and BYOL) with and without margins as well as two other components; emphasizing positive samples (in short *pos.*), weighting positive samples differently (abbreviated as *curv.*). We tested each model in two different settings; linear probing (Tab. 3) and transfer learning (Tab. 4). It is worth noting that the optimal value of s depends on the SSL method across datasets. Furthermore, across all SSL methods and datasets, the optimal value of c typically lies between 0.7 and 2.5. Experimental details, including exact values of s and c , are addressed in the supplementary.

Tabs. 3 and 4 present the linear probing and transfer learning performance on four datasets. In addition, Tab. 1 shows the linear probing performance on ImageNet. As indicated in Tab. 3, the most significant improvement of MoCo occurs when positive samples are emphasized. The transfer learning performance (Tab. 4) demonstrates that this performance improvement is not due to overfitting but rather reflects enhanced representations capable of generalizing to unseen datasets. While *curv.* coupled with *pos.* can improve performance in seen datasets, it does not consistently enhance performance in unseen datasets. SimCLR and BYOL do not exhibit significant performance improvements across the four datasets, in contrast to MoCo. As mentioned in Sec. 5.2, emphasizing positive samples does not significantly improve SimCLR. However, considering the results on ImageNet (Tab. 1) and its increased batch size, it is anticipated that increasing the batch size provides more opportunities to emphasize positive samples, leading to significant improvement. BYOL is structurally less affected by margins or their associated effects. Consequently, performance improvements are limited, except when pretrained on TinyImageNet. In conclusion, optimizing margins and related effects can contribute to performance enhancements on the target dataset, and emphasizing positive samples appears to be crucial for achieving improved representations that generalize to unseen datasets.

6 Limitations and Discussion

Our work is based on several assumptions; cosine similarity and one-hot target probability p_{ij} . Various forms of contrastive learning algorithms, such as MoCo, SimCLR, BYOL, and SwAV, do not violate these assumptions [20, 5, 17, 3]. Yet, since not all methods follow these assumptions, our work requires further validation to determine whether the observations made in this study can be transferred to other contrastive learning methods that violate these assumptions [10, 40].

7 Conclusion

We analyzed the gradients of InfoNCE loss with margins and found that margins induce a mixture of three different effects: emphasizing positive samples, weighting positive samples differently based on their angles, and alleviating the diminishing gradient effect as the estimated probability approaches the target probability. We separated each effect and experimentally demonstrated the significance and limits of each. Additionally, we discovered that maximizing each component separately can perform better than controlling the mixture of effects through margins. We hope our analysis of how margins affect the gradients of representation learning will help improve self-supervised learning.

References

- [1] Baldi, P. and Hornik, K. Neural networks and principal component analysis: Learning from examples without local minima. *Neural Networks*, 2(1):53–58, 1989. ISSN 0893-6080. doi: [https://doi.org/10.1016/0893-6080\(89\)90014-2](https://doi.org/10.1016/0893-6080(89)90014-2).
- [2] Boutros, F., Damer, N., Kirchbuchner, F., and Kuijper, A. Elasticface: Elastic margin loss for deep face recognition. In *Proceedings of the IEEE/CVF Conference on Computer Vision and Pattern Recognition (CVPR) Workshops*, pp. 1578–1587, 6 2022.
- [3] Caron, M., Misra, I., Mairal, J., Goyal, P., Bojanowski, P., and Joulin, A. Unsupervised learning of visual features by contrasting cluster assignments. In Larochelle, H., Ranzato, M., Hadsell, R., Balcan, M. F., and Lin, H. (eds.), *Advances in Neural Information Processing Systems*, volume 33, pp. 9912–9924. Curran Associates, Inc., 2020. SwAV.
- [4] Chen, M., Radford, A., Child, R., Wu, J., Jun, H., Luan, D., and Sutskever, I. Generative pretraining from pixels. In *Proceedings of the 37th International Conference on Machine Learning, ICML’20*. JMLR.org, 2020.
- [5] Chen, T., Kornblith, S., Norouzi, M., and Hinton, G. A simple framework for contrastive learning of visual representations. In III, H. D. and Singh, A. (eds.), *Proceedings of the 37th International Conference on Machine Learning*, volume 119, pp. 1597–1607. PMLR, 9 2020. SimCLR.
- [6] Chen, T., Kornblith, S., Swersky, K., Norouzi, M., and Hinton, G. E. Big self-supervised models are strong semi-supervised learners. In Larochelle, H., Ranzato, M., Hadsell, R., Balcan, M. F., and Lin, H. (eds.), *Advances in Neural Information Processing Systems*, volume 33, pp. 22243–22255. Curran Associates, Inc., 2020. SimCLRv2.
- [7] Chen, X. and He, K. Exploring simple siamese representation learning. In *Proceedings of the IEEE/CVF Conference on Computer Vision and Pattern Recognition (CVPR)*, pp. 15750–15758, 6 2021. SimSIAM.
- [8] Chen, X., Fan, H., Girshick, R., and He, K. Improved baselines with momentum contrastive learning. *arXiv preprint arXiv:2003.04297*, 2020.
- [9] Chen, X., Xie, S., and He, K. An empirical study of training self-supervised vision transformers. In *Proceedings of the IEEE/CVF International Conference on Computer Vision (ICCV)*, pp. 9640–9649, 10 2021.
- [10] Chuang, C.-Y., Robinson, J., Lin, Y.-C., Torralba, A., and Jegelka, S. Debaised contrastive learning. In Larochelle, H., Ranzato, M., Hadsell, R., Balcan, M., and Lin, H. (eds.), *Advances in Neural Information Processing Systems*, volume 33, pp. 8765–8775. Curran Associates, Inc., 2020.
- [11] Coates, A., Ng, A., and Lee, H. An analysis of single-layer networks in unsupervised feature learning. In *Proceedings of the fourteenth international conference on artificial intelligence and statistics*, pp. 215–223. JMLR Workshop and Conference Proceedings, 2011.
- [12] Deng, J., Guo, J., Xue, N., and Zafeiriou, S. Arcface: Additive angular margin loss for deep face recognition. In *Proceedings of the IEEE/CVF conference on computer vision and pattern recognition*, pp. 4690–4699, 2019.
- [13] Desplanques, B., Thienpondt, J., and Demuynck, K. ECAPA-TDNN: Emphasized Channel Attention, Propagation and Aggregation in TDNN Based Speaker Verification. In *Proc. Interspeech 2020*, pp. 3830–3834, 2020. doi: 10.21437/Interspeech.2020-2650.
- [14] Devlin, J., Chang, M., Lee, K., and Toutanova, K. BERT: pre-training of deep bidirectional transformers for language understanding. In *Proceedings of the 2019 Conference of the North American Chapter of the Association for Computational Linguistics: Human Language Technologies, NAACL-HLT 2019, Minneapolis, MN, USA, June 2-7, 2019, Volume 1 (Long and Short Papers)*, pp. 4171–4186. Association for Computational Linguistics, 2019.

- [15] Doersch, C., Gupta, A., and Efros, A. A. Unsupervised visual representation learning by context prediction. In *Proceedings of the IEEE international conference on computer vision*, pp. 1422–1430, 2015.
- [16] Dosovitskiy, A., Beyer, L., Kolesnikov, A., Weissenborn, D., Zhai, X., Unterthiner, T., Dehghani, M., Minderer, M., Heigold, G., Gelly, S., Uszkoreit, J., and Housby, N. An image is worth 16x16 words: Transformers for image recognition at scale. In *International Conference on Learning Representations*, 2021.
- [17] Grill, J.-B., Strub, F., Altché, F., Tallec, C., Richemond, P., Buchatskaya, E., Doersch, C., Pires, B. A., Guo, Z., Azar, M. G., Piot, B., koray kavukcuoglu, Munos, R., and Valko, M. Bootstrap your own latent - a new approach to self-supervised learning. In Larochelle, H., Ranzato, M., Hadsell, R., Balcan, M. F., and Lin, H. (eds.), *Advances in Neural Information Processing Systems*, volume 33, pp. 21271–21284. Curran Associates, Inc., 2020. BYOL.
- [18] HaoChen, J. Z., Wei, C., Gaidon, A., and Ma, T. Provable guarantees for self-supervised deep learning with spectral contrastive loss. In Ranzato, M., Beygelzimer, A., Dauphin, Y., Liang, P., and Vaughan, J. W. (eds.), *Advances in Neural Information Processing Systems*, volume 34, pp. 5000–5011. Curran Associates, Inc., 2021. URL https://proceedings.neurips.cc/paper_files/paper/2021/file/27debb435021eb68b3965290b5e24c49-Paper.pdf.
- [19] He, K., Zhang, X., Ren, S., and Sun, J. Deep residual learning for image recognition. In *Proceedings of the IEEE Conference on Computer Vision and Pattern Recognition (CVPR)*, June 2016.
- [20] He, K., Fan, H., Wu, Y., Xie, S., and Girshick, R. Momentum contrast for unsupervised visual representation learning. In *Proceedings of the IEEE/CVF Conference on Computer Vision and Pattern Recognition (CVPR)*, 6 2020. MoCo.
- [21] Hermans, A., Beyer, L., and Leibe, B. In defense of the triplet loss for person re-identification. *arXiv preprint arXiv:1703.07737*, 2017.
- [22] Hsu, W.-N., Bolte, B., Tsai, Y.-H. H., Lakhota, K., Salakhutdinov, R., and Mohamed, A. Hubert: Self-supervised speech representation learning by masked prediction of hidden units. *IEEE/ACM Transactions on Audio, Speech, and Language Processing*, 29:3451–3460, 2021.
- [23] Huang, Y., Wang, Y., Tai, Y., Liu, X., Shen, P., Li, S., Li, J., and Huang, F. Curricularface: Adaptive curriculum learning loss for deep face recognition. In *Proceedings of the IEEE/CVF Conference on Computer Vision and Pattern Recognition (CVPR)*, 6 2020.
- [24] Kim, M., Jain, A. K., and Liu, X. Adaface: Quality adaptive margin for face recognition. In *Proceedings of the IEEE/CVF Conference on Computer Vision and Pattern Recognition (CVPR)*, pp. 18750–18759, 6 2022.
- [25] Krizhevsky, A., Hinton, G., et al. Learning multiple layers of features from tiny images, 2009.
- [26] Le, Y. and Yang, X. Tiny imagenet visual recognition challenge. *CS 231N*, 7(7):3, 2015.
- [27] Meng, Q., Zhao, S., Huang, Z., and Zhou, F. Magface: A universal representation for face recognition and quality assessment. In *Proceedings of the IEEE/CVF Conference on Computer Vision and Pattern Recognition (CVPR)*, pp. 14225–14234, 6 2021.
- [28] Mikolov, T., Sutskever, I., Chen, K., Corrado, G. S., and Dean, J. Distributed representations of words and phrases and their compositionality. *Advances in neural information processing systems*, 26, 2013.
- [29] Oord, A. v. d., Li, Y., and Vinyals, O. Representation learning with contrastive predictive coding. *arXiv preprint arXiv:1807.03748*, 2018.
- [30] Pathak, D., Krahenbuhl, P., Donahue, J., Darrell, T., and Efros, A. A. Context encoders: Feature learning by inpainting. In *Proceedings of the IEEE conference on computer vision and pattern recognition*, pp. 2536–2544, 2016.

- [31] Russakovsky, O., Deng, J., Su, H., Krause, J., Satheesh, S., Ma, S., Huang, Z., Karpathy, A., Khosla, A., Bernstein, M., Berg, A. C., and Fei-Fei, L. Imagenet large scale visual recognition challenge. *Int. J. Comput. Vision*, 115(3):211–252, dec 2015. ISSN 0920-5691. doi: 10.1007/s11263-015-0816-y. URL <https://doi.org/10.1007/s11263-015-0816-y>.
- [32] Wang, F. and Liu, H. Understanding the behaviour of contrastive loss. In *Proceedings of the IEEE/CVF Conference on Computer Vision and Pattern Recognition (CVPR)*, pp. 2495–2504, June 2021.
- [33] Wang, H., Wang, Y., Zhou, Z., Ji, X., Gong, D., Zhou, J., Li, Z., and Liu, W. Cosface: Large margin cosine loss for deep face recognition. In *Proceedings of the IEEE Conference on Computer Vision and Pattern Recognition (CVPR)*, 6 2018.
- [34] Wang, H., Guo, X., Deng, Z.-H., and Lu, Y. Rethinking minimal sufficient representation in contrastive learning. In *Proceedings of the IEEE/CVF Conference on Computer Vision and Pattern Recognition (CVPR)*, pp. 16041–16050, 6 2022.
- [35] Wu, Z., Xiong, Y., Yu, S. X., and Lin, D. Unsupervised feature learning via non-parametric instance discrimination. In *Proceedings of the IEEE conference on computer vision and pattern recognition*, pp. 3733–3742, 2018.
- [36] Yu, Y., Chan, K. H. R., You, C., Song, C., and Ma, Y. Learning diverse and discriminative representations via the principle of maximal coding rate reduction. In Larochelle, H., Ranzato, M., Hadsell, R., Balcan, M., and Lin, H. (eds.), *Advances in Neural Information Processing Systems*, volume 33, pp. 9422–9434. Curran Associates, Inc., 2020.
- [37] Zhan, F., Yu, Y., Wu, R., Zhang, J., Lu, S., and Zhang, C. Marginal contrastive correspondence for guided image generation. In *Proceedings of the IEEE/CVF Conference on Computer Vision and Pattern Recognition (CVPR)*, pp. 10663–10672, 6 2022.
- [38] Zhang, A., Ma, W., Wang, X., and Chua, T.-S. Incorporating bias-aware margins into contrastive loss for collaborative filtering. In Oh, A. H., Agarwal, A., Belgrave, D., and Cho, K. (eds.), *Advances in Neural Information Processing Systems*, 2022. URL <https://openreview.net/forum?id=apC354ZsGwK>.
- [39] Zhang, X., Zhao, R., Qiao, Y., Wang, X., and Li, H. Adacos: Adaptively scaling cosine logits for effectively learning deep face representations. In *Proceedings of the IEEE/CVF Conference on Computer Vision and Pattern Recognition (CVPR)*, 6 2019.
- [40] Zheng, M., You, S., Wang, F., Qian, C., Zhang, C., Wang, X., and Xu, C. Rssl: Relational self-supervised learning with weak augmentation. In Ranzato, M., Beygelzimer, A., Dauphin, Y., Liang, P. S., and Vaughan, J. W. (eds.), *Advances in Neural Information Processing Systems*, volume 34, pp. 2543–2555. Curran Associates, Inc., 2021.

A Proofs

A.1 Subtractive margin

Eq. 11 can be rewritten as follows:

$$\begin{aligned} \frac{\partial \mathcal{L}_i}{\partial \theta_{ij}} &= (p_{ij} - \beta q_{ij}) \frac{\sin(\theta_{ij} + m_1 p_{ij})}{\tau} = \frac{-\beta \exp(\delta_{ij}) + p_{ij} \sum_{k \in \mathcal{X}} \exp(\delta_{ik})}{\sum_{k \in \mathcal{X}} \exp(\delta_{ik})} \frac{\sin(\theta_{ij} + m_1 p_{ij})}{\tau} \\ &= \frac{-\beta \exp(\delta_{ij}) + p_{ij} \sum_{k \in \mathcal{X}} \exp(\delta_{ik})}{\sum_{k \in \mathcal{X}} \exp(\hat{\delta}_{ik})} \frac{\sum_{k \in \mathcal{X}} \exp(\hat{\delta}_{ik})}{\sum_{k \in \mathcal{X}} \exp(\delta_{ik})} \frac{\sin(\theta_{ij} + m_1 p_{ij})}{\tau}. \end{aligned} \quad (22)$$

$\hat{\delta}_{ij}$ denotes logits without subtractive margin m_2 . We use the fact that $\exp(\delta_{ij})$ equals $\exp(\hat{\delta}_{ij}) \exp(-m_2 p_{ij} / \tau)$. For brevity, we will use the notation η_{ij} for $\exp(-m_2 p_{ij} / \tau)$. We can rewrite as follows;

$$\frac{\partial \mathcal{L}_i}{\partial \theta_{ij}} = \frac{-\beta \exp(\hat{\delta}_{ij}) \eta_{ij} + p_{ij} \sum_{k \in \mathcal{X}} \exp(\hat{\delta}_{ik}) \eta_{ik}}{\sum_{k \in \mathcal{X}} \exp(\hat{\delta}_{ik})} \frac{\sum_{k \in \mathcal{X}} \exp(\hat{\delta}_{ik})}{\sum_{k \in \mathcal{X}} \exp(\hat{\delta}_{ik}) \eta_{ik}} \frac{\sin(\theta_{ij} + m_1 p_{ij})}{\tau}. \quad (24)$$

We further assume that there are only one positive sample and other samples are negative. This assumption holds true for SSL methods we are analyzing. We will use l to denote the index of a positive sample. Furthermore, we use the fact that η_{ih} of negative sample h equals one. We can further simplify the equation using this assumption as follows;

$$\frac{\partial \mathcal{L}_i}{\partial \theta_{ij}} = \frac{-\beta \exp(\hat{\delta}_{ij}) \eta_{ij} + p_{ij} (\exp(\hat{\delta}_{il}) (\eta_{il} - 1) + \sum_{k \in \mathcal{X}} \exp(\hat{\delta}_{ik}))}{\sum_{k \in \mathcal{X}} \exp(\hat{\delta}_{ik})} \frac{\sum_{k \in \mathcal{X}} \exp(\hat{\delta}_{ik})}{\sum_{k \in \mathcal{X}} \exp(\hat{\delta}_{ik}) \eta_{ij}} \frac{\sin(\theta_{ij} + m_1 p_{ij})}{\tau} \quad (25)$$

$$= (p_{ij} + \frac{-\beta \exp(\hat{\delta}_{ij}) \eta_{ij} + p_{ij} \exp(\hat{\delta}_{il}) (\eta_{il} - 1)}{\sum_{k \in \mathcal{X}} \exp(\hat{\delta}_{ik})}) \frac{\sum_{k \in \mathcal{X}} \exp(\hat{\delta}_{ik})}{\sum_{k \in \mathcal{X}} \exp(\hat{\delta}_{ik}) \eta_{ij}} \frac{\sin(\theta_{ij} + m_1 p_{ij})}{\tau} \quad (26)$$

$$= (p_{ij} - \beta \hat{q}_{ij} \eta_{ij} + p_{ij} \hat{q}_{il} (\eta_{il} - 1)) \frac{\sum_{k \in \mathcal{X}} \exp(\hat{\delta}_{ik})}{\sum_{k \in \mathcal{X}} \exp(\hat{\delta}_{ik}) \eta_{ij}} \frac{\sin(\theta_{ij} + m_1 p_{ij})}{\tau} \quad (27)$$

$$= (p_{ij} - \beta \hat{q}_{ij} \eta_{ij} + p_{ij} \hat{q}_{il} (\eta_{il} - 1)) \frac{\sum_{k \in \mathcal{X}} \exp(\hat{\delta}_{ik})}{\exp(\hat{\delta}_{il}) (\eta_{il} - 1) + \sum_{k \in \mathcal{X}} \exp(\hat{\delta}_{ik})} \frac{\sin(\theta_{ij} + m_1 p_{ij})}{\tau} \quad (28)$$

$$= (p_{ij} - \beta \hat{q}_{ij} \eta_{ij} + p_{ij} \hat{q}_{il} (\eta_{il} - 1)) \frac{1}{1 - (1 - \eta_{il}) \hat{q}_{il}} \frac{\sin(\theta_{ij} + m_1 p_{ij})}{\tau}. \quad (29)$$

Under the assumption that β to one (which holds true for MoCo and SimCLR), gradients for a positive sample l can be rewritten as follows;

$$\frac{\partial \mathcal{L}_i}{\partial \theta_{il}} = (p_{il} + \hat{q}_{il} (p_{il} (\eta_{il} - 1) - \beta \eta_{il})) \frac{1}{1 - (1 - \eta_{il}) \hat{q}_{il}} \frac{\sin(\theta_{il} + m_1 p_{il})}{\tau} \quad (30)$$

$$= (p_{il} - \hat{q}_{il}) \frac{\sin(\theta_{il} + m_1 p_{il})}{\tau} \frac{1}{1 - (1 - \eta_{il}) \hat{q}_{il}}. \quad (31)$$

Similarly, by using η_{ih} equals one, we can get the gradients for a negative sample h as follows;

$$\frac{\partial \mathcal{L}_i}{\partial \theta_{ih}} = (p_{ih} - \beta \hat{q}_{ih} \eta_{ih}) \frac{1}{1 - (1 - \eta_{il}) \hat{q}_{il}} \frac{\sin(\theta_{il} + m_1 p_{ih})}{\tau} \quad (32)$$

$$= (p_{ih} - \hat{q}_{ih}) \frac{\sin(\theta_{il} + m_1 p_{ih})}{\tau} \frac{1}{1 - (1 - \eta_{il}) \hat{q}_{il}}. \quad (33)$$

That is, under the above assumptions, subtractive margin multiplies both positive and negative sample gradients by $1/(1 - (1 - \eta_{il})\hat{q}_{il})$.

Table 5: Margin values for four datasets (Tab. 3).

Method	Dataset	$m1$	$m2$
<i>MoCov3</i>	CIFAR10	0.1	0.4
	CIFAR100	0.5	0.7
	STL10	0.4	0.6
	TinyImageNet	0.1	0.4
<i>SimCLR</i>	CIFAR10	0.5	0.4
	CIFAR100	0.6	0.6
	STL10	0.0	0.2
	TinyImageNet	0.0	0.8

Table 6: Scaling factors of *pos.* only models.

Method	Dataset	<i>pos.</i> (s)
<i>MoCov3</i>	CIFAR10	20
	CIFAR100	20
	STL10	40
	TinyImageNet	20
<i>SimCLR</i>	CIFAR10	1.125
	CIFAR100	1.0625
	STL10	1.0625
	TinyImageNet	1.0625

Table 7: Scaling factors and curvature factors.

Method	Dataset	<i>pos.</i> (s)	<i>curv.</i> (c)
<i>MoCov3</i>	CIFAR10	20	0.7
	CIFAR100	40	1
	STL10	40	2.5
	TinyImageNet	40	2.5
<i>SimCLR</i>	CIFAR10	2.5	0.7
	CIFAR100	2	0.7
	STL10	1.25	0.7
	TinyImageNet	1.125	1.0
<i>BYOL</i>	CIFAR10	-	1.0
	CIFAR100	-	2.5
	STL10	-	5.0
	TinyImageNet	-	2.5

B Implementation Details

B.1 Experimental settings for CIFAR-10, CIFAR-100, STL-10, and TinyImageNet

Our experimental settings for these dataset basically follows that of ReSSL. We pretrained each model on a source dataset for 200 epochs and then fine-tuned it on a target dataset for 100 epochs. We set the batch size to 256 and τ to 0.25 (for MoCov3 and SimCLR). The latent feature dimension was set to 128, while the hidden dimension of linear layers (including projection heads and predictors) was set to 2048. We used SGD with a momentum of 0.9 for both pretraining and evaluation. The learning rate was set to 0.06 for pretraining the backbone model and 1 for fine-tuning the linear layer. During evaluation, we employed the cosine annealing learning rate scheduler.

We used two augmentation policies: strong and weak augmentation. The strong augmentation consists of random resize cropping, horizontal flipping, color jittering, random gray scaling, and Gaussian blurring. In contrast, the weak augmentation only included random horizontal and random cropping. For contrastive learning-based SSL methods with a teacher model (MoCov3, BYOL), we used weak data augmentation to the teacher model and strong data augmentation to the student model. For a method without a teacher model (SimCLR), however, we use these two different augmentation policies to generate two different representations of the same identity.

For projection heads and predictors of MoCov3, SimCLR, and BYOL, we used batch normalization before the ReLU activation.

During hyperparameter tuning for comparison with baselines, we only adjusted margins (m_1 and m_2), s (Eq.17), and c (Eq.19), while keeping other hyperparameters fixed, such as the learning rate. The hyperparameters used in Sec. 5.5 are specified in Tabs. 5, 7 and 6.

B.2 Experimental settings for ImageNet

We used the official implementations of both MoCov3 and SimCLR. Due to our computational budget, we pretrained the networks for 100 epochs. Following the experimental settings of MoCov3 and SimCLR, we fine-tuned the last linear layer for 90 epochs for evaluation. We only modified the gradient scales using Alg. 3, without making any other changes. When training SimCLR, we used a two-linear layered projection module. This choice was made because only the official performance of the two-linear-layered version, pretrained for 100 epochs, was available. For both MoCo and SimCLR, we use a batch size of 4,096.

The hyperparameters (s and c), used in Tab. 1 are as follows: for MoCov3, we set s to 10 and c to 1.5, while for SimCLR, s was set to 2 and c to 1.

C Pseudo code

In this section, we provide pseudo codes for reproduction. Although contrastive learning-based baselines do not explicitly utilize angles, as mentioned in the main paper, computing logits using cosine similarity can be interpreted as obtaining logits using the angles that result from taking the arccos of the cosine similarity values (Alg. 1). We used Alg. 2 to use margins in contrastive learning methods. To modify the gradient scale, it can be accomplished by replacing only the process of converting angles to logits from Alg. 1 to Algs.3, 4, and 5. As the algorithms demonstrate, our modification does not affect the logit values but solely modifies the gradients. To adjust the curvature of positive gradient scales in BYOL, it suffices to set p as an all-ones vector since only positive samples are used.

Algorithm 1 Logits as a function of angles: pseudo code of general contrastive learning (Eq. 4)

Inputs:

θ Angles
 τ Temperature

$logits \leftarrow \cos(\theta)/\tau$

return $logits$

Algorithm 2 Logits with margins (m_1 and m_2) (Eq. 7)

Inputs:

θ Angles
 τ Temperature
 p Target probabilities
 m_1 Angular margin
 m_2 Subtractive margin

$logits \leftarrow (\cos(\theta + p \times m_1) - p \times m_2)/\tau$

return $logits$

Algorithm 3 Emphasizing positive samples and controlling the curvature of positive gradient scales (Fig. 5, Tabs. 1 and 3).

Inputs:

θ Angles
 τ Temperature
 p Target probabilities
 s Scaling factor
 c Curvature factor

$logits \leftarrow \cos(\theta)/\tau$

$scales \leftarrow stop_gradient(s \times (1 - \frac{\theta}{\pi})^{1/c})$

$logits \leftarrow (1 - p) \times logits + p \times ((\frac{1}{\pi} - scales) \times stop_gradient(logits) + scales \times logits)$

return $logits$

Algorithm 4 Attenuating the diminishing gradients (Type I) (Eq. 20)

Inputs:

θ Angles
 τ Temperature
 p Target probabilities
 α Attenuation factor

$logits \leftarrow \cos(\theta)/\tau$

$q \leftarrow softmax(logits)$

$scales \leftarrow sum(p/stop_gradient(p - \alpha \times q), dim = -1)$

$logits \leftarrow (1 - scales) \times stop_gradient(logits) + scales \times logits$

return $logits$

Algorithm 5 Attenuating the diminishing gradients of positive samples (Type II) (Eq. 21)

Inputs:

θ Angles
 τ Temperature
 p Target probabilities
 α Attenuation factor

$logits \leftarrow \cos(\theta)/\tau$

$q \leftarrow softmax(logits)$

$scales \leftarrow 1/stop_gradient(p - \alpha \times q)$

$logits \leftarrow (1 - p) \times logits + p \times ((1 - scales) \times stop_gradient(logits) + scales \times logits)$

return $logits$
